Rapid Communications

Exactly solvable Majorana-Anderson impurity models

G. Shankar[1] and J. Maciejko[1,2,3]

[1]*Department of Physics, University of Alberta, Edmonton, Alberta, Canada T6G 2E1*

[2]*Theoretical Physics Institute, University of Alberta, Edmonton, Alberta, Canada T6G 2E1*

[3]*Canadian Institute for Advanced Research, Toronto, Ontario, Canada M5G 1Z8*

(Received 4 June 2019; revised manuscript received 16 September 2019; published 12 December 2019)

Motivated by recent experimental progress in the realization of hybrid structures with a topologically superconducting nanowire coupled to a quantum dot, viewed through the lens of the emerging field of correlated Majorana fermions, we introduce a class of interacting Majorana-Anderson impurity models which admit an exact solution for a wide range of parameters, including on-site repulsive interactions of arbitrary strength. The model is solved by mapping it via the $\mathbb{Z}_2$ slave-spin method to a noninteracting resonant level model for auxiliary Majorana degrees of freedom. The resulting gauge constraint is eliminated by exploiting the transformation properties of the Hamiltonian under a special local particle-hole transformation. For a spin-polarized Kitaev chain coupled to a quantum dot, we obtain exact expressions for the dot spectral functions at both zero and finite temperature. We study how the interaction strength and localization length of the end Majorana zero mode affect the physical properties of the dot, such as the quasiparticle weight, double occupancy, and odd-frequency pairing correlations, as well as the local electronic density of states in the superconducting chain.

DOI: 10.1103/PhysRevB.100.241105

Introduction. The discovery of topological phases of quantum matter has led to a paradigm shift in condensed matter physics. The simplest such topological phase, the one-dimensional (1D) topological superconductor (SC) [1], hosts localized Majorana zero modes (MZMs) at its ends which can form a topological qubit immune to decoherence, with exciting prospects for quantum computation [2,3]. Strong evidence suggests MZMs have been observed in experiments on proximitized semiconductor nanowires [4] and ferromagnetic chains [5], following specific theoretical proposals [5–7].

On the theoretical front, a new direction has emerged which explores the interplay of pure MZM physics, well understood from single-particle quantum mechanics, and electronic correlations [8]. Recently studied lattice models of interacting MZMs such as the Majorana-Hubbard [9–14] and Majorana-Falicov-Kimball [15,16] models may be relevant to describe Abrikosov vortex lattices in 2D topological SCs [17], where each vortex hosts an unpaired MZM [18,19]. Motivated by transport experiments on proximitized nanowires, another avenue of research has explored interacting Anderson-type quantum impurity models involving small numbers of MZMs coupled to dissipative baths, some of which are predicted to exhibit exotic Kondo effects [20–22]. A geometry of particular interest, that of an end MZM tunnel-coupled to a quantum dot (QD), is now experimentally accessible [23] and argued to directly probe the nonlocality of MZMs [24–30]. Existing theoretical studies of this problem have largely relied on mean-field approximations [27,28,30] or numerical methods [26,27] to treat correlation effects in the corresponding Anderson model [31]. Such studies also typically model the MZM as a unique on-site Majorana operator, whereas the MZM localization length is generically finite, as known from both theory [1] and experiment [32]. In this Rapid Communication, we introduce a class of Majorana-Anderson impurity (MAI) models which admit an exact solution regardless of interaction strength and the degree of MZM localization.

Majorana-Anderson impurity models and exact solvability. We consider a class of models described by a lattice Hamiltonian of the form $H = H_C + H_A + H_{\rm hyb}$, where H_C describes either a host material or leads that couple to the QD, and is quadratic in spinless fermion operators $c_j, c_j^\dagger$ where j is a site index. The QD is modeled as an Anderson impurity,

$$H_A = U\prod_\sigma(2n_{d\sigma}-1) + \frac{\epsilon}{2}(n_{d\uparrow}+n_{d\downarrow}-1) - \frac{h}{2}(n_{d\uparrow}-n_{d\downarrow}), \tag{1}$$

where $n_{d\sigma} = d_\sigma^\dagger d_\sigma$ is the number operator for fermions of spin $\sigma \in \{\uparrow,\downarrow\}$ on the impurity. U describes on-site Coulomb repulsion, h is a Zeeman field, and ϵ is a shift in the chemical potential of the impurity fermions. The hybridization between the host and QD is

$$H_{\rm hyb} = -i\sum_j V_j(c_j + c_j^\dagger)(d_\uparrow + d_\uparrow^\dagger), \tag{2}$$

which allows for the possibility of spatially extended hybridization (strength V_j) between the QD and host. This form of Majorana hybridization arises naturally if the host supports a localized MZM that is in proximity to an impurity. As MZMs arise in effectively spin-polarized SCs, it is reasonable to expect that only one impurity spin species will hybridize [26–28,33]. The number $n_{d\downarrow}$ of spin-$\downarrow$ fermions being thus conserved, the problem studied here can be thought of as a Majorana version of the x-ray edge problem [34,35]. By contrast with the classic Nozières–De Dominicis solution of the original problem [35], which is restricted to asymptotically low frequencies, here we find an exact solution for the impurity spectral functions at all frequencies.

The key ingredient in constructing an exact solution for the MAI model is the $\mathbb{Z}_2$ slave-spin method pioneered by Rüegg *et al.* [36,37] and since employed in a variety of contexts ranging from non-Fermi liquids [38] to fractionalized topological phases [39–42] and the Mott transition in infinite dimensions [43]. Following Ref. [36], we fractionalize the physical impurity fermions into an Ising slave pseudospin and slave fermions as $d_\sigma^{(\dagger)} = \mu^x f_\sigma^{(\dagger)}$, where $\sigma \in \{\uparrow, \downarrow\}$ is the spin projection (along $\hat{z}$) of the physical (d) and slave (f) fermions, and $\{\mu^x, \mu^y, \mu^z\}$ are Pauli matrices that describe the auxiliary slave pseudospin. Physical states in the enlarged Hilbert space satisfy the gauge constraint

$$\mu^z = 2(n_f - 1)^2 - 1, \tag{3}$$

where $n_f = f_\uparrow^\dagger f_\uparrow + f_\downarrow^\dagger f_\downarrow$ is the total number of slave fermions. The constraint can be used to construct a projector,

$$\mathbb{P} = \tfrac{1}{2}[1 + (-1)^{n_f}\mu^z], \tag{4}$$

that projects onto the physical subspace. The slave-spin (SS) representation of H in the physical subspace is then

$$H_{\rm SS} = H_C - i\sum_j V_j(c_j + c_j^\dagger)(f_\uparrow + f_\uparrow^\dagger)\mu^x + U\mu^z + \frac{1}{2}[\epsilon + h + (\epsilon - h)\mu^z](n_{f\downarrow} - 1/2), \tag{5}$$

where the constraint equation has been used to rewrite the interaction, chemical potential, and Zeeman terms [44]. Defining new Majorana operators $\Gamma_\uparrow^\alpha = \mu^\alpha(f_\uparrow + f_\uparrow^\dagger)$ where $\alpha \in \{x, y, z\}$, and using $\mu^z = -i\mu^x\mu^y = -i\Gamma_\uparrow^x\Gamma_\uparrow^y$, the slave-spin Hamiltonian can be written entirely in terms of fermion operators as

$$H_{\rm SS} = H_C - i\sum_j V_j(c_j + c_j^\dagger)\Gamma_\uparrow^x - iU\Gamma_\uparrow^x\Gamma_\uparrow^y + \frac{1}{2}[\epsilon + h - i(\epsilon - h)\Gamma_\uparrow^x\Gamma_\uparrow^y](n_{f\downarrow} - 1/2). \tag{6}$$

For $\epsilon = h$, this model is bilinear in fermions and thus exactly solvable. Henceforth, we set $\epsilon = h$, and consider deviations from this exactly solvable limit later. In an experimental situation we expect ϵ and h to be tunable via gate potentials and applied magnetic fields, respectively.

The physical partition function for MAI models can be computed in the SS representation without constraint, even away from the exactly solvable point. The proof is similar to those for other such constraint-free models studied using the $\mathbb{Z}_2$ slave-spin method [15,43–45]. Defining a particle-hole transformation $\mathcal{D}_\uparrow$ that acts only on $d_\uparrow$ as $\mathcal{D}_\uparrow d_\uparrow \mathcal{D}_\uparrow^{-1} = d_\uparrow^\dagger$, Eqs. (1) and (2) yield $\mathcal{D}_\uparrow H(V, U, \epsilon, h)\mathcal{D}_\uparrow^{-1} = H(V, -U, h, \epsilon)$. Since the partition function is invariant under similarity transformations of the Hamiltonian, $\mathcal{Z}(V, U, \epsilon, h) = \mathcal{Z}(V, -U, h, \epsilon)$. This transformation is implemented in the SS representation (on $H_{\rm SS}$) by μ^x. Using cyclicity of the trace and the relation $\mu^x\mathbb{P}\mu^x = 1 - \mathbb{P}$, it is easy to show that $\mathcal{Z} = \mathcal{Z}_{\rm SS}/2$. Similarly, it can also be shown that correlation functions of operators that commute with $\mathcal{D}_\uparrow$ are calculable without constraint [46]. However, for MAI models, it is possible to exactly implement the constraint and compute *all* correlation functions in the SS representation. To see this, note that the projector $\mathbb{P}$ admits a fermion representation,

$$\mathbb{P} = i\Gamma_\uparrow^z\gamma'_{f\uparrow}(f_\downarrow^\dagger f_\downarrow - 1/2) + 1/2, \tag{7}$$

where $\gamma'_{f\uparrow} = -i(f_\uparrow - f_\uparrow^\dagger)$. A (time-ordered) correlation function G of a physical operator O that is not invariant under the particle-hole transformation $\mathcal{D}_\uparrow$ must be calculated in the SS representation *with* the projector,

$$G = 2\langle\hat{T}_\tau O_{\rm SS}(\tau_1)O_{SS}(\tau_2)\mathbb{P}\rangle_{\rm SS}, \tag{8}$$

where $O_{\rm SS}$ is the SS representation of the physical operator O. The factor of 2 is because $\mathcal{Z} = \mathcal{Z}_{\rm SS}/2$. As the expectation value on the right-hand side (RHS) is taken with respect to the quadratic slave-spin Hamiltonian $H_{\rm SS}$, Wick's theorem can be used to explicitly implement $\mathbb{P}$ and calculate G exactly.

Impurity edge-coupled to the Kitaev chain. As an application and concrete demonstration of our results, we now specialize to the case of an impurity hybridizing with the end of a semi-infinite Kitaev chain [1]. This special case is hereafter referred to as the KMAI (Kitaev Majorana-Anderson impurity) model. The SS representation of the KMAI model is obtained by using $H_C = H_K$ and $V_i = V\delta_{i1}$ in Eq. (6), where

$$H_K = \sum_{j=1}^{\infty}[(-tc_j^\dagger c_{j+1} + \Delta c_j c_{j+1} + \text{H.c.}) - \mu c_j^\dagger c_j] \tag{9}$$

describes a semi-infinite Kitaev chain with a hopping integral t, p-wave pairing amplitude Δ, and chemical potential μ. The physical Green's functions (GFs) for $d_\downarrow$ ($d_\uparrow$), calculable without (with) constraint, are obtained in the SS representation as a product of free-fermion imaginary-time slave GFs. For example, the $d_\downarrow$-fermion GF is given by

$$\mathcal{G}_{d\downarrow}(\tau) = -\langle\hat{T}_\tau\Gamma_\uparrow^y(\tau)\Gamma_\uparrow^y(0)\Gamma_\uparrow^z(\tau)\Gamma_\uparrow^z(0)f_\downarrow(\tau)f_\downarrow^\dagger(0)\rangle_{\rm SS}, \tag{10}$$

where the RHS can be Wick contracted. In the Matsubara frequency domain, this becomes a convolution product, which after analytic continuation to real frequencies gives rise to temperature (T) dependence in the spectral functions of the physical impurity fermions (d_σ). This emphasizes that the latter are interacting, even though the slave fermions are not. The one-particle slave-fermion GFs appearing on the RHS of Eq. (10) after Wick contraction can be calculated exactly using boundary GF methods [46]. When $\epsilon = 0$, H enjoys full particle-hole (ph) symmetry and $\mathcal{G}_{d\downarrow}$ is T independent and given by

$$\mathcal{G}_{d\downarrow}^{\rm ph}(ik_n) = \frac{ik_n - 2V^2 g_{\gamma_1}(ik_n)}{(ik_n)^2 - 4U^2 - 2ik_nV^2 g_{\gamma_1}(ik_n)}, \tag{11}$$

where $g_{\gamma_1}(\tau) = -\langle\hat{T}_\tau\gamma_1(\tau)\gamma_1(0)\rangle$, with $\gamma_1 = c_1 + c_1^\dagger$, is the boundary GF of the semi-infinite Kitaev chain in the absence of an impurity. Away from particle-hole symmetry, $\mathcal{G}_{d\downarrow}(ik_n)$ can only be given an integral expression, but the spectral function has a simple form,

$$A_{d\downarrow}(\omega, T) = 2[1 - 2n_F(\epsilon)]\{n_B(\epsilon)n_F(\omega - \epsilon) + [n_B(\epsilon) + 1][1 - n_F(\omega - \epsilon)]\}A_{d\downarrow}^{\rm ph}(\omega - \epsilon), \tag{12}$$

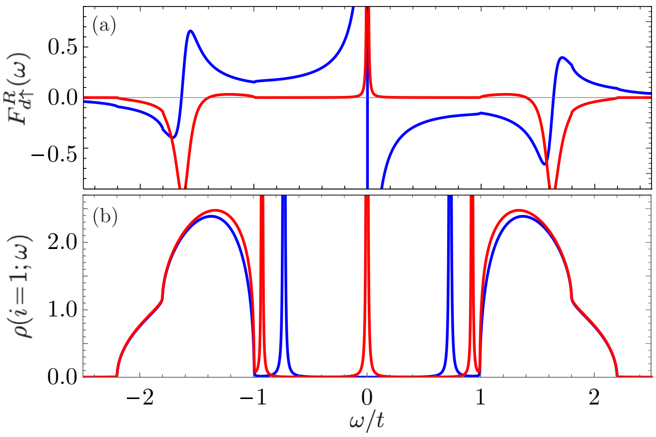

FIG. 1. (a) Real (blue) and imaginary (red) parts of the impurity retarded Gor'kov function $F^R_{d\uparrow}(\omega)$ for a Kitaev chain in the topological phase. Parameters are chosen as $\mu = 0.2t$, $\Delta = 0.5t$, $V = 0.4t$, $U = 0.7t$. (b) Interaction dependence of the boundary density of states $\rho(i = 1, \omega)$ of the c fermions, for $\mu = 0.2t$, $\Delta = 0.5t$, $V = 0.4t$, and $U = 0$ (blue), $U = 0.3t$ (red).

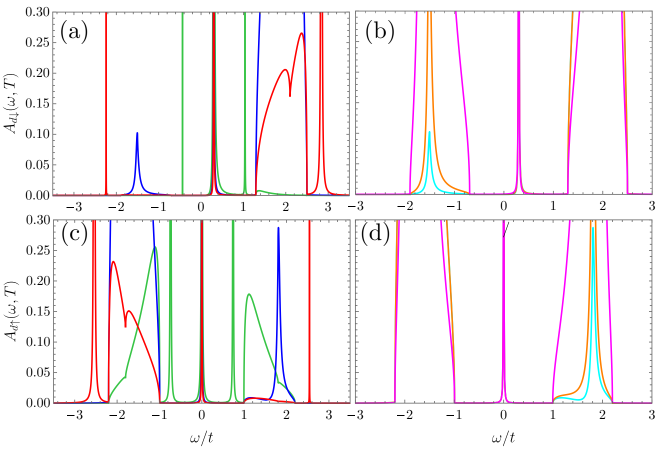

FIG. 2. (a)–(d) Spectral functions of $d_\downarrow$ (top row) and $d_\uparrow$ (bottom row) for various interaction strengths U (left column) and temperatures T (right column), shown in the topological phase. In all plots, $\mu = 0.2t$, $\Delta = 0.5t$, $V = 0.4t$, $\epsilon = 0.3t$ are fixed. Left column: $T = 0.05t$ and $U = 0.05t$ (green), $U = 0.8t$ (blue), $U = 1.2t$ (red). Right column: $U = 0.8t$ and $T = 0.05t$ (cyan), $T = 0.07t$ (orange), $T = t$ (magenta).

where $A^{\rm ph}_{d\downarrow}(\omega)$ is the T-independent, particle-hole symmetric spectral function obtained from Eq. (11), and n_B (n_F) is the Bose (Fermi) function. The first term in Eq. (12) corresponds to the absorption of a spin-↑ bosonic density fluctuation of energy ϵ by a spin-↓ fermion of energy $\omega - \epsilon$, while the second term describes the emission, stimulated or spontaneous, of such a density fluctuation by a fermion of energy ω. Turning now to the hybridizing $d_\uparrow$ impurity fermion, its Matsubara GF can be calculated by explicitly implementing the projector $\mathbb{P}$ using Eq. (7), which yields

$$\mathcal{G}_{d\uparrow}(ik_n) = \frac{ik_n - V^2 g_{\gamma_1}(ik_n) + 2U[2n_F(\epsilon) - 1]}{(ik_n)^2 - 4U^2 - 2ik_n V^2 g_{\gamma_1}(ik_n)}. \qquad (13)$$

An expression for $A_{d\uparrow}(\omega, T)$ can be obtained from the analytic continuation of Eq. (13) to real frequencies.

Odd-frequency pairing. The Majorana hybridization with the Kitaev chain results in proximity-induced superconductivity for the $d_\uparrow$ fermions. The only possibility in this case is pure odd-frequency pairing [47], characterized by the real (imaginary) part of the retarded Gor'kov function being odd (even) in frequency [48–50] [Fig. 1(a)]. The latter is obtained by analytic continuation of the Matsubara Gor'kov function,

$$\mathcal{F}_{d\uparrow}(ik_n) = \frac{V^2 g_{\gamma_1}(ik_n)}{(ik_n)^2 - 4U^2 - 2ik_n V^2 g_{\gamma_1}(ik_n)}, \qquad (14)$$

where $g_{\gamma_1}(ik_n)$ is odd in ik_n by virtue of being a Majorana GF [51,52]. Odd-frequency pairing on the impurity is a consequence of the particle-hole symmetric form (2) of the hybridization term, and in fact obtains regardless of the specific host Hamiltonian H_C.

Impurity spectral functions. We now turn to the spectral functions $A_{d\sigma}(\omega)$ of the impurity fermions, and restrict our discussion to the topological phase of the KMAI model. The deviation ϵ from the particle-hole symmetric point sets the scale for the interaction-induced temperature dependence of those spectral functions. Low temperatures and $\epsilon > 0$ accentuate the spectral asymmetry in $A_{d\downarrow}$ about $\omega = \epsilon$, shifting the spectral weight towards excitations with $\omega > \epsilon$. It can be seen from Eq. (12) that, in the limit $T \gg \epsilon$, the temperature-dependent prefactors tend towards unity, and particle-hole symmetry is restored [Fig. 2(b)]. This behavior with respect to temperature can be intuitively understood in the atomic limit ($V = 0$). In this limit, there are two infinitely sharp peaks in $A_{d\downarrow}$ at $\omega_\pm = \epsilon \pm 2U$ corresponding to localized charge excitations on the impurity. The spectral weight for ω_+ is greater as it is proportional to the $d_\uparrow$-fermion occupancy $\langle n_{d\uparrow}\rangle$, which is favored over $d_\downarrow$-fermion occupancy for $\epsilon > 0$. Flipping the sign of ϵ reverses this asymmetry, for $d_\downarrow$-fermion occupancy is then favored. This behavior with respect to temperature carries over to the case when $V \neq 0$. The temperature dependence of $A_{d\uparrow}$ can also be similarly explained.

When the hybridization V and interaction U are both nonzero, both impurity GFs have three poles (in the topological phase) which manifest as quasiparticle peaks in their spectral functions [Figs. 2(a) and 2(c)]. The two side peaks correspond to impurity charge excitations, with a gap that increases monotonically with U. For small U and V, these excitations feature as sharp peaks inside the energy gap of the Kitaev SC. As U or V is increased, they fall into the SC energy bands and broaden, and then eventually again become sharp peaks when they move out of the bandwidth of the SC. That the gap grows monotonically with U is expected, as these states differ in charge/occupancy.

The third quasiparticle peak (at $\omega = \epsilon$ for $A_{d\downarrow}$ and $\omega = 0$ for $A_{d\uparrow}$) is never broadened and persists for any nonzero U, V. We consider the $\omega = \epsilon$ peak in $A_{d\downarrow}$. This is where a sharp peak would occur were the $d_\downarrow$ free ($U = 0$), but it is not and the peak persists for large U. This is an indirect signature of the presence of an MZM, as can be understood from the small U/V limit. A semi-infinite Kitaev chain implies there must be an exact MZM at zero energy. But the original MZM $(c_1 + c_1^\dagger)$ of the Kitaev chain is now paired with $d_\uparrow + d_\uparrow^\dagger$ to form a local complex fermion due to $H_{\rm hyb}$. Neither of the two

Majorana modes that make up $d_\downarrow$ can be the new MZM as $n_{d\downarrow}$ is conserved. Therefore, $-i(d_\uparrow - d_\uparrow^\dagger)$ must be the new MZM in the small-U/V limit. As it has to be an exact zero mode, interactions cannot change its energy. In this limit, the $d_\downarrow$ becomes free, and this features as a sharp peak in $A_{d\downarrow}$ at $\omega = \epsilon$. That $-i(d_\uparrow - d_\uparrow^\dagger)$ is the preferred MZM in this limit features as a sharp peak at $\omega = 0$ in $A_{d\uparrow}$. In the opposite large-U/V limit, energetics suggest that the original mode $(c_1 + c_1^\dagger)$ is the preferred MZM.

An obvious check of this intuitive reasoning is provided by the c-fermion local density of states (LDOS) at the boundary—there must be an MZM peak at any finite U, with spectral weight that *increases* with U. The local GFs for the c-fermions can be calculated on an arbitrary lattice site [46], from which the corresponding LDOS can be obtained. The boundary LDOS [Fig. 1(b)] supports our intuition: An MZM peak appears for any nonzero interaction and its spectral weight obtained by numerical integration does increase with U. The two other subgap states are nontopological Andreev bound states induced by the impurity, reminiscent of Yu-Shiba-Rusinov states [53–55].

Local Fermi liquid. Since the free-fermion peak in $A_{d\downarrow}$ remains sharp even in the presence of interactions, a natural quantity to study is the associated quasiparticle weight Z. This can be calculated from Eqs. (11) and (12) and is given by

$$Z = \frac{1}{1 + (2/\lambda)(U/V)^2}, \tag{15}$$

where $\lambda(\mu, \Delta)$ is the spectral weight (characterizing the localization) of the MZM peak in the boundary LDOS of a noninteracting Kitaev chain with no impurity [46]. In the noninteracting limit, the $d_\downarrow$ fermion is free and so $Z = 1$. The interaction renormalizes Z to a value less than one [Fig. 3(a)], and transfers some spectral weight to other excitations, thus giving credence to a *local Fermi-liquid* picture for the $d_\downarrow$ fermion. This holds only in the topological phase, as the free-fermion peak for finite U and V has its origins in $-i(d_\uparrow - d_\uparrow^\dagger)$ being an MZM candidate, which is not true in the trivial phase. It is also not valid for the hybridizing $d_\uparrow$ fermion, as the spectral weight of the $\omega = 0$ peak is trivially less than one due to proximity coupling with the Kitaev chain, even in the absence of interactions. Also, conforming with the intuitive discussion in the previous section, Z is suppressed at large U, when $c_1 + c_1^\dagger$ is the preferred MZM.

Another measure of interparticle correlations on the QD is provided by the mean-squared density fluctuation $D = (1/2)\langle(n_d - \langle n_d\rangle)^2\rangle$, where $n_d = n_{d\uparrow} + n_{d\downarrow}$. In the particle-hole symmetric limit ($\epsilon = 0$), because $\langle n_d\rangle = 1$ this reduces to the double occupancy $D = \langle n_{d\uparrow} n_{d\downarrow}\rangle$, which can be calculated from a derivative of the logarithm of the partition function with respect to U, to get

$$D = \frac{1}{4} + \frac{U}{2}\int \frac{d\omega}{2\pi} A_{(d+d^\dagger)\uparrow}(\omega)\frac{n_F(\omega)}{\omega}, \tag{16}$$

where $A_{(d+d^\dagger)\uparrow}(\omega)$ is the spectral function of the hybridizing Majorana mode $d_\uparrow + d_\uparrow^\dagger$. The Matsubara GF of this operator is simply the sum of electron, hole, and Gor'kov GFs of the $d_\uparrow$ fermion. Plots of D [Fig. 3(b)] reveal that density fluctuations are suppressed at large U and low T, but encouraged by hybridization V.

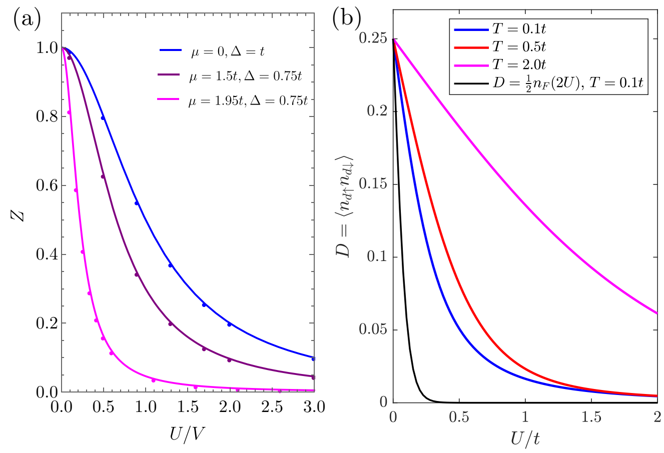

FIG. 3. (a) Interaction dependence of the $d_\downarrow$-fermion quasiparticle weight Z, for several values of μ and Δ, which control the localization length of the original end MZM in the Kitaev chain. Continuous curves correspond to Eq. (15), while dots are the result of numerically integrating $A_{d\downarrow}(\omega, T)$ over a small neighborhood of $\omega = \epsilon$. (b) Interaction dependence of impurity double occupancy D for various T in the particle-hole symmetric limit ($\epsilon = 0$). Black: Atomic limit ($V = 0$); all other curves: $\mu = 0.2t$, $\Delta = 0.5t$, $V = 0.4t$, $\epsilon = 0$.

Departures from exact solvability. We now consider deviations from the exactly solvable point $\epsilon = h$. Defining $\delta = (\epsilon - h)/2$, the SS Hamiltonian (6) becomes

$$H_{\rm SS} = H_{\rm SS}(\epsilon = h) - \delta(n_{f\downarrow} - 1/2) - i\delta\Gamma_\uparrow^x\Gamma_\uparrow^y(n_{f\downarrow} - 1/2), \tag{17}$$

where $H_{\rm SS}(\epsilon = h)$ is the bilinear exactly solvable part. For sufficiently small δ, corrections to physical observables away from the exactly solvable limit can be computed by treating the last term in Eq. (17) in perturbation theory, in analogy to the perturbative analysis of small departures from the Toulouse point in the Kondo problem [56]. We emphasize that this is distinct from ordinary perturbation theory in the physical interaction strength U; here, U can be arbitrarily large, and the perturbation corresponds to either a shift in the chemical potential of the impurity fermions or a change in the Zeeman field. For example, to linear order in δ, the free energy is $F = F^{(0)} + F^{(1)}\delta + O(\delta^2)$, where

$$F^{(1)} = 2[1 - 2n_F(\epsilon)][1/4 - D] - n_F(\epsilon), \tag{18}$$

with D the T-dependent double occupancy in the particle-hole symmetric limit, given in Eq. (16).

Outlook. Several extensions of our work are possible. Besides different choices of the bath Hamiltonian, such as 2D or 3D topological SCs or Majorana hopping models, our exact solution trivially generalizes to periodic Majorana-Anderson models, where the impurity fermions acquire a lattice-site index. However, the $\mathbb{Z}_2$ slave-spin solution of such models involves a local projection on every site, as in the Majorana-Falicov-Kimball model [15], which likely limits exact solvability to the computation of correlation functions of operators that commute with the local particle-hole transformation $\mathcal{D}_\uparrow$ [see Eq. (8)]. While applications to spin-polarized topological SCs naturally justify a spin-selective choice (2) of the hybridization term [26–28,33], it is also possible to generalize the latter such that multiple Majorana modes on the QD hybridize equally with the bath fermions while retaining exact solvability.

Acknowledgments. We thank R. Boyack for helpful discussions. J.M. was supported by NSERC Grant No. RGPIN-2014-4608, the CRC Program, CIFAR, and the University of Alberta.

[1] A. Yu. Kitaev, Phys. Usp. **44**, 131 (2001).
[2] A. Yu. Kitaev, Ann. Phys. (N.Y.) **303**, 2 (2003).
[3] C. Nayak, S. H. Simon, A. Stern, M. Freedman, and S. Das Sarma, Rev. Mod. Phys. **80**, 1083 (2008).
[4] V. Mourik, K. Zuo, S. M. Frolov, S. R. Plissard, E. P. A. M. Bakkers, and L. P. Kouwenhoven, Science **336**, 1003 (2012).
[5] S. Nadj-Perge, I. K. Drozdov, J. Li, H. Chen, S. Jeon, J. Seo, A. H. MacDonald, B. A. Bernevig, and A. Yazdani, Science **346**, 602 (2014).
[6] R. M. Lutchyn, J. D. Sau, and S. Das Sarma, Phys. Rev. Lett. **105**, 077001 (2010).
[7] Y. Oreg, G. Refael, and F. von Oppen, Phys. Rev. Lett. **105**, 177002 (2010).
[8] For a recent review, see A. Rahmani and M. Franz, Rep. Prog. Phys. **82**, 084501 (2019).
[9] A. Rahmani, X. Zhu, M. Franz, and I. Affleck, Phys. Rev. Lett. **115**, 166401 (2015); Phys. Rev. B **92**, 235123 (2015).
[10] I. Affleck, A. Rahmani, and D. Pikulin, Phys. Rev. B **96**, 125121 (2017).
[11] C. Li and M. Franz, Phys. Rev. B **98**, 115123 (2018).
[12] K. Wamer and I. Affleck, Phys. Rev. B **98**, 245120 (2018).
[13] A. Rahmani, D. Pikulin, and I. Affleck, Phys. Rev. B **99**, 085110 (2019).
[14] T. Hayata and A. Yamamoto, Phys. Rev. B **96**, 035129 (2017).
[15] C. Prosko, S.-P. Lee, and J. Maciejko, Phys. Rev. B **96**, 205104 (2017).
[16] X.-H. Li, Z. Chen, and T.-K. Ng, Phys. Rev. B **100**, 094519 (2019).
[17] C.-K. Chiu, D. I. Pikulin, and M. Franz, Phys. Rev. B **91**, 165402 (2015).
[18] N. Read and D. Green, Phys. Rev. B **61**, 10267 (2000).
[19] L. Fu and C. L. Kane, Phys. Rev. Lett. **100**, 096407 (2008).
[20] B. Béri and N. R. Cooper, Phys. Rev. Lett. **109**, 156803 (2012).
[21] A. Altland and R. Egger, Phys. Rev. Lett. **110**, 196401 (2013).
[22] L. Herviou, K. Le Hur, and C. Mora, Phys. Rev. B **94**, 235102 (2016).
[23] M. T. Deng, S. Vaitiekėnas, E. B. Hansen, J. Danon, M. Leijnse, K. Flensberg, J. Nygård, P. Krogstrup, and C. M. Marcus, Science **354**, 1557 (2016).
[24] M. Leijnse and K. Flensberg, Phys. Rev. B **84**, 140501(R) (2011).
[25] D. E. Liu and H. U. Baranger, Phys. Rev. B **84**, 201308(R) (2011).
[26] M. Lee, J. S. Lim, and R. López, Phys. Rev. B **87**, 241402(R) (2013).
[27] M. Cheng, M. Becker, B. Bauer, and R. M. Lutchyn, Phys. Rev. X **4**, 031051 (2014).
[28] D. E. Liu, M. Cheng, and R. M. Lutchyn, Phys. Rev. B **91**, 081405(R) (2015).
[29] D. J. Clarke, Phys. Rev. B **96**, 201109(R) (2017).
[30] E. Prada, R. Aguado, and P. San-Jose, Phys. Rev. B **96**, 085418 (2017).
[31] In Ref. [27] an exact solution was presented, but for an effective Kondo model to which the Anderson model reduces in the limit of infinite on-site repulsion $U \to \infty$ on the QD, in which charge fluctuations are completely frozen out. By contrast, our exactly solvable model keeps U finite and retains the degrees of freedom associated with charge fluctuations.
[32] S. M. Albrecht, A. P. Higginbotham, M. Madsen, F. Kuemmeth, T. S. Jespersen, J. Nygård, P. Krogstrup, and C. M. Marcus, Nature (London) **531**, 206 (2016).
[33] S. Hoffman, D. Chevallier, D. Loss, and J. Klinovaja, Phys. Rev. B **96**, 045440 (2017).
[34] G. D. Mahan, Phys. Rev. **153**, 882 (1967).
[35] P. Nozières and C. T. De Dominicis, Phys. Rev. **178**, 1097 (1969).
[36] A. Rüegg, S. D. Huber, and M. Sigrist, Phys. Rev. B **81**, 155118 (2010).
[37] S. D. Huber and A. Rüegg, Phys. Rev. Lett. **102**, 065301 (2009).
[38] R. Nandkishore, M. A. Metlitski, and T. Senthil, Phys. Rev. B **86**, 045128 (2012).
[39] A. Rüegg and G. A. Fiete, Phys. Rev. Lett. **108**, 046401 (2012).
[40] J. Maciejko and A. Rüegg, Phys. Rev. B **88**, 241101(R) (2013).
[41] J. Maciejko, V. Chua, and G. A. Fiete, Phys. Rev. Lett. **112**, 016404 (2014).
[42] D. Prychynenko and S. D. Huber, Physica B (Amsterdam) **481**, 53 (2016).
[43] R. Žitko and M. Fabrizio, Phys. Rev. B **91**, 245130 (2015).
[44] D. Guerci, Phys. Rev. B **99**, 195409 (2019).
[45] D. Guerci and M. Fabrizio, Phys. Rev. B **96**, 201106(R) (2017).
[46] See Supplemental Material at http://link.aps.org/supplemental/10.1103/PhysRevB.100.241105 for an explicit proof of the disappearance of the slave-spin constraint as well as details regarding the calculation of boundary GFs in the KMAI model, which includes Refs. [15,57,58].
[47] S.-P. Lee, R. M. Lutchyn, and J. Maciejko, Phys. Rev. B **95**, 184506 (2017).
[48] V. L. Berezinskii, JETP Lett. **20**, 287 (1974).
[49] T. R. Kirkpatrick and D. Belitz, Phys. Rev. Lett. **66**, 1533 (1991).
[50] A. Balatsky and E. Abrahams, Phys. Rev. B **45**, 13125 (1992).
[51] Y. Asano and Y. Tanaka, Phys. Rev. B **87**, 104513 (2013).
[52] Z. Huang, P. Wölfle, and A. V. Balatsky, Phys. Rev. B **92**, 121404(R) (2015).
[53] L. Yu, Acta Phys. Sin. **21**, 75 (1965).
[54] H. Shiba, Prog. Theor. Phys. **40**, 435 (1968).
[55] A. I. Rusinov, Sov. Phys. JETP **29**, 1101 (1969).
[56] P. B. Wiegmann and A. M. Finkelstein, Sov. Phys. JETP **48**, 102 (1978).
[57] T. Jonckheere, J. Rech, A. Zazunov, R. Egger, and T. Martin, Phys. Rev. B **95**, 054514 (2017).
[58] A. Umerski, Phys. Rev. B **55**, 5266 (1997).